

This discussion paper is/has been under review for the journal Atmospheric Measurement Techniques (AMT). Please refer to the corresponding final paper in AMT if available.

Chemistry of α -pinene and naphthalene oxidation products generated in a Potential Aerosol Mass (PAM) chamber as measured by acetate chemical ionization mass spectrometry

P. S. Chhabra¹, A. T. Lambe^{1,2}, M. R. Canagaratna¹, H. Stark^{1,3}, J. T. Jayne¹, T. B. Onasch^{1,2}, P. Davidovits², J. R. Kimmel^{1,3,4}, and D. R. Worsnop¹

¹Aerodyne Research, Inc. Billerica, Massachusetts, USA

²Chemistry Department, Boston College, Chestnut Hill, Massachusetts, USA

³Cooperative Institute for Research in Environmental Sciences (CIRES), University of Colorado, Boulder, Colorado, USA

⁴TOFWERK AG, Thun, Switzerland

Received: 19 May 2014 – Accepted: 12 June 2014 – Published: 1 July 2014

Correspondence to: P. S. Chhabra (puneet@aerodyne.com)

Published by Copernicus Publications on behalf of the European Geosciences Union.

6385

Abstract

Recent developments in high resolution, time-of-flight chemical ionization mass spectrometry (HR-ToF-CIMS) have made possible the direct detection of atmospheric organic compounds in real-time with high sensitivity and with little or no fragmentation, including low volatility, highly oxygenated organic vapors that are precursors to secondary organic aerosol formation. Here, for the first time, we examine gas-phase O₃ and OH oxidation products of α -pinene and naphthalene formed in the PAM flow reactor with an HR-ToF-CIMS using acetate reagent ion chemistry. Integrated OH exposures ranged from 1.2×10^{11} to 9.7×10^{11} molec cm⁻³ s, corresponding to approximately 1.0 to 7.5 days of equivalent atmospheric oxidation. Measured gas-phase organic acids are similar to those previously observed in environmental chamber studies. For both precursors, we find that acetate-CIMS spectra capture both functionalization (oxygen addition) and fragmentation (carbon loss) as a function of OH exposure. The level of fragmentation is observed to increase with increased oxidation. We present a method that estimates vapor pressures of organic molecules using the measured O/C ratio, H/C ratio, and carbon number for each compound detected by the CIMS. The predicted condensed-phase SOA average acid yields and O/C and H/C ratios agree within uncertainties with previous AMS measurements and ambient CIMS results. While acetate reagent ion chemistry is used to selectively measure organic acids, in principle this method can be applied to additional reagent ion chemistries depending on the application.

1 Introduction

Oxygenated organics are an abundant class of compounds in the atmosphere, representing significant fractions of the total organic mass in the gas, particle, and cloud droplet phases (Goldstein and Galbally, 2007; Zhang et al., 2007; Jimenez et al., 2009). Much of the oxygenated organic mass is secondary in origin, generated from the

6386

gas-phase oxidation (O_3 , $OH/HO_2/NO_x$, NO_3) of anthropogenic and biogenic volatile organic compounds (VOCs) (Kroll and Seinfeld, 2008; Seinfeld and Pandis, 2006; Goldstein and Galbally, 2007). Recent studies have shown that secondary organic aerosol oxygen content is correlated with the photochemical age of an air mass (Ng et al., 2011; Heald et al., 2010; Jimenez et al., 2009). With increasing oxidation, gas-phase organic compounds can partition into the particle phase to contribute to SOA mass or into the aqueous phase to contribute to water soluble organic carbon (WSOC) (Hallquist et al., 2009; Ervens et al., 2011; Lim et al., 2010). As a result, their potential impact on climate by increasing and changing the properties of total aerosol mass and cloud condensation nuclei is substantial. However, sources, processing, and sinks of atmospheric organics are poorly characterized owing to their vast chemical complexity (Goldstein and Galbally, 2007). As a result, there is significant uncertainty in modeled secondary organic aerosol loadings and chemistries (Spracklen et al., 2011; Hallquist et al., 2009; Dzepina et al., 2011), necessitating more comprehensive measurements of gas- and particle-phase organics and better predictions of their SOA forming potentials.

Mass spectrometry has become a ubiquitous tool in identifying and quantifying atmospherically relevant organic species. Further, high-resolution mass spectrometry has increasingly become an important technique in elucidating the composition of organics because of its ability to resolve high molecular weight compounds with the same nominal mass with high sensitivity. Offline methods like electrospray ionization coupled with ultrahigh-resolution mass spectrometry are useful in identifying the many different compounds extracted from aerosol filter collection (Laskin et al., 2012; Kundu et al., 2012; Putman et al., 2012) as well as fog samples (Mazzoleni et al., 2010). Such methods, however, are highly selective with variable sensitivities and are not typically suited for online or field measurements. Conversely, the widely used Aerodyne high-resolution time-of-flight aerosol mass spectrometer (HR-ToF-AMS) couples electron ionization with the TOFWERK (Thun, Switzerland) high-resolution time-of-flight mass spectrometer (HTOF) to provide sensitive, quantitative, online measurements of organic aerosol

6387

elemental composition (Jayne et al., 2000; Canagaratna et al., 2007; DeCarlo et al., 2006; Aiken et al., 2007). The harsh electron ionization of the HR-ToF-AMS limits its speciation capability and introduces uncertainty in its elemental ratio calculation (Chhabra et al., 2011; Farmer et al., 2010; Aiken et al., 2008). Thus, improvements to high-resolution mass spectrometry of atmospherically relevant high molecular weight compounds have sought to combine fast online detection with soft ionization sources (Zahardis et al., 2011).

Recently, the TOFWERK HTOF has been paired with various chemical ionization sources to allow for the sensitive detection of organic compounds at high time resolutions (≤ 1 s) with little to no molecular fragmentation. Chemical ionization sources employ specific reagent ions to initiate reactions that ionize analyte species; different reagent ions tend to be selective to different classes of compounds. The use of acetate chemical ionization mass spectrometry (acetate-CIMS) as a way to quantitatively measure organic acids was first demonstrated by Veres et al. (2008) using a quadrupole mass spectrometer. Veres et al. (2010) used the acetate-CIMS technique to measure acids of carbon number (n_C) 1 to 4, benzenediols, and inorganic acids from biomass burning, and Veres et al. (2011) used acetate-CIMS to measure small organic acids produced in urban air. Bertram et al. (2011) first described the use of a low mass resolution ($R = 900$) time-of-flight CIMS which, unlike the quadrupole mass spectrometer, could acquire whole mass spectra at high time resolutions. Yatavelli et al. (2012) demonstrated the potential of a high mass resolution (HTOF, $R = 4000$) acetate-CIMS to measure a large range ($1 \geq n_C \geq 30$) of organic acids in both particle and gas phases from α -pinene ozonolysis and subsequently used it in a remote forest atmosphere (Yatavelli et al., 2014). Aside from traditional organic acids the technique has also been used to measure water-soluble organics compounds (WSOC) generated from α -pinene ozonolysis (Aljawhary et al., 2013) and nitrophenols from biomass burning (Mohr et al., 2013). The ability of the HTOF to acquire whole mass spectra at high time and mass resolutions represents a substantial improvement over quadrupole technology.

6388

As soft ionization time-of-flight mass spectrometry techniques become more widely used to study gas- and aerosol-phase organics, methods will be needed to relate the many different species depicted in complex mass spectral data to the physical properties of the detected species. Volatility, expressed as vapor pressure, p^0 , or saturated mass concentration, c^* , is an important property that governs whether a species partitions into the condensed phase. There has been much effort to relate HR-AMS data to volatility; thermal denuder measurements and dilution experiments with the AMS have been used to constrain the volatility of organic aerosol (Cappa and Jimenez, 2010; Cappa, 2010; Huffman et al., 2009). The lack of carbon number information from AMS data, a key input in volatility prediction models, may produce uncertainty. Soft ionization high-resolution mass spectrometry retains full molecular information in its spectra, i.e. the chemical formula, $C_xH_yO_z$, of unfragmented parent molecules can be obtained. Thus it has the potential to provide the inputs for more accurate volatility estimations.

In this study, we explore the high-resolution acetate-CIMS spectra of photochemically produced organic acids and predict the volatility of the species detected. Acids are of particular interest because carboxylic acid functionality dramatically reduces the vapor pressure of its parent molecule and also represents the oxidative endpoint for a terminal carbon before fragmentation. Carboxylic acids also contribute a significant portion of total SOA mass (Ng et al., 2011; Vogel et al., 2013). We choose to examine the α -pinene, and naphthalene systems because their gas-phase compositions and mechanisms have been studied in detail, and various acids have been identified in each system (Yu et al., 1999; Claeys et al., 2013; Kautzman et al., 2009). Using the Van Krevelen diagram (hydrogen-to carbon ratio, H/C, plotted against the oxygen-to-carbon ratio, O/C) and Kroll diagram (oxidation state, OS_C plotted vs. carbon number, n_C), we identify small organic acids and tracer compounds and examine the changing distributions of carbon as a function of OH-exposure for the first time using the Potential Aerosol Mass (PAM) flow reactor. We note that while the HR-ToF-CIMS can detect many different mass-to-charge ions, the exact quantification of the concentration of these identified compounds requires the calibration for many individual species which

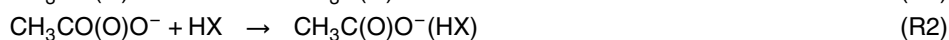
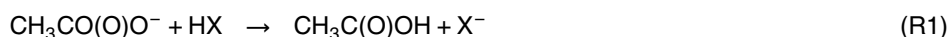
6389

can be impractical. This will be an on going developmental issue with the HR-ToF-CIMS systems. Our approach is to use a sensitivity value and the uncertainty it introduces will be discussed. Additionally, we develop an algorithm to estimate the volatility of the species detected in each system and discuss the implications of the results.

2 Experimental method and data analysis

2.1 Acetate-CIMS

The Aerodyne HR-ToF-CIMS, hereby referred to as the CIMS, using acetate reagent ion chemistry has been described in detail in previous publications (Bertram et al., 2011; Yatavelli et al., 2012). Sample from the PAM reactor is drawn through a critical orifice at 2.0 L min^{-1} into the ion-molecular reaction (IMR) chamber. Acetate reagent ions are generated by bubbling approximately 200 sccm of N_2 through a reservoir of acetic anhydride, diluting the flow to 2 L min^{-1} with N_2 and passing it through a commercial ^{210}Po alpha emitter (P-2021, NRD) before introducing it into the IMR orthogonally to the sample flow (Veres et al., 2008). Within the IMR, acetate ions abstract protons from acids having gas-phase acidities greater than that of acetic acid or cluster with gas-phase species to form adduct ions, as shown in Reactions (R1) and (R2).



The IMR (100 mbar) is coupled to the HTOF mass analyzer (1×10^{-7} mbar) by a series of differentially pumped stages that includes DC and RF focusing optics (AP interface). The first pumping stage contains a segmented, RF-only quadrupole operated at 2 mbar. Voltages in this quadrupole can be tuned to transmit (weak field) or dissociate (strong field) or non-covalent clusters. In these experiments, voltages were adjusted in order to minimize the clustering, as indicated by the by the signal at m/z 119 (acetic

6390

corresponding to the α -pinene ozonolysis spectrum presented in Fig. 2a. Markers are numbered and colored by n_C , sized by the ion signal intensity, and weighted by n_C to emphasize the distribution of carbon across the spectra. Identified ions with known chemical formulae are marked with gray circles and squares in Fig. 3a (squares: (Yu et al., 1999); circles: (Claeys et al., 2013); names and structures are given in Fig. S3 in the Supplement). Figure 3a illustrates those ions with $n_C = 1$ to 12 are measured by the acetate-CIMS for α -pinene ozonolysis. Much of the carbon ($\sim 46\%$) is characterized by molecules with O/C = 0.3 to 0.7 and $n_C = 7$ to 10, including ions corresponding to well-characterized gas-phase oxidation products such as $C_{10}H_{16}O_3$ (pinic acid) and norpinonic acid ($C_{10}H_{14}O_3$), which by themselves contribute $\sim 14\%$ of the measured carbon. Other $n_C = 10$ ions are also detected, with O/C values as high as 0.7 such as $C_{10}H_{16}O_7$ and $C_{10}H_{14}O_7$. Highly oxidized ions with these formulas have been previously measured by Ehn et al. (2012) in ambient and chamber experiments. The acids identified by Yu et al. (1999) contribute approximately 20% to the measured carbon of acidic α -pinene ozonolysis products. Acids identified by Claeys et al. (2013) such as 3-methyl-1,2,3-butanetricarboxylic acid (MBTCA, $C_8H_{12}O_6$) and terebic acid ($C_7H_{10}O_4$) have smaller contributions on the order of $\sim 3\%$.

Approximately 31% of the carbon is contained in small highly oxidized acids with $n_C = 1$ to 3 and O/C ≥ 1 . Because the relative abundance of these acids increases as a function of OH exposure they are presumably formed following fragmentation of early-generation oxidation products with larger n_C . Small- n_C ions with large signals include CH_2O_2 (formic acid), $C_2H_2O_3$ (glyoxylic acid), and $C_3H_4O_3$ (pyruvic acid) which represent 26% of the total carbon measured for α -pinene ozonolysis products. We measured a formic acid molar yield of 10%, which is similar to the molar yield of $7.5 \pm 0.7\%$ reported by Lee et al. (2006).

The Van Krevelen diagram of naphthalene is shown in Fig. 3b. Measured naphthalene oxidation products that have been observed in previous chamber studies (depicted by gray square boxes, structures and names given in Fig. S4 in the Supplement) represent at most 33% of the carbon and include $C_8H_6O_3$ (phthalaldehydic acid), $C_8H_6O_4$

6399

(phthalic acid), and $C_{10}H_8O_3$ (formylcinnamic acid) (Kautzman et al., 2009). We measured several oxidation products with $n_C = 9$ and 10, including $C_9H_6O_4$ and $C_{10}H_8O_5$ that to our knowledge have not been previously identified. In naphthalene spectra, a strong $C_4H_5O_4$ ion signal was detected that corresponds to a previously unidentified compound. Two possible structures are (1) a diacid with two saturated, unoxygenated carbons, or (2) a mono-acid with one double bond and two hydroxyl groups, which may be more plausible.

3.3 Oxidation state vs. carbon number

Figure 4 displays oxidation state as a function of carbon number for α -pinene and naphthalene oxidation products as a function of OH exposure. The utility of plotting OS_C as a function of n_C (i.e. Kroll Diagram) was introduced by Kroll et al. (2011) to provide a visualization of the chemical complexity of atmospheric organics and their corresponding oxidation trajectories. The top inset panels show the fraction of carbon signal as a function of n_C . A multimodal n_C distribution is observed for α -pinene and naphthalene oxidation products (Fig. 4a and b top insets). The mode defined by $n_C = 8$ –10 species can be viewed as “functionalized” products where a net addition of oxygen occurs while the carbon backbone of the precursor is mostly retained (Lambe et al., 2012; Kroll et al., 2009). Figure 4a and b shows that the fraction of acids with $n_C = 8$ –10 decrease as a function of OH exposure. The fact that this decrease is directly correlated with an increase in the fraction of acids with $n_C < 4$ suggests that the $n_C < 4$ species are largely produced by fragmentation processes in which carbon-carbon bond cleavage occurs during oxidation of the $n_C = 8$ –10 species.

Several other precursor-specific features are evident from Fig. 4. First, as is illustrated by the marker size in the main panel and curves in the right panel, CIMS signals peak at OH exposures of 3.7×10^{11} and 7.0×10^{11} molec cm⁻³ s for naphthalene and α -pinene oxidation products, respectively. Second, the carbon distribution of naphthalene oxidation products has negligible contributions from molecules with $n_C = 3, 5$, and 6. This is because naphthalene is unlikely to form pyruvic acid, an $n_C = 3$ acid with

6400

production of small acids formed from the fragmentation of a larger carbon backbone. The H/C ratios of α -pinene gas-phase products are lower than those of the particle-phase suggesting that the gas-phase acids might have more carbonyl groups and thus carbon with a higher oxidation state than carbon in the particle phase. In contrast, the H/C ratios of naphthalene gas-phase products are higher than those of the particle-phase indicating that oxidation and fragmentation increase the oxidation state of carbon relative to carbon in aromatic rings. Particularly, the difference suggests that the particle phase is dominated by aromatic ring-retaining products while the gas phase is dominated by non-aromatic acid fragmentation products. The elemental ratios of the gas-phases products from both precursors display a convergence with increased OH exposure indicating the predominance of the same $n_C = 1-4$ acids, especially glyoxylic and glycolic acids.

Figure 8 also shows average O/C and H/C ratios of ambient organic aerosols measured with an acetate-MOVI-HRToF-CIMS during the BEACHON-RoMBAS field campaign (Yatavelli et al., 2014; Ortega et al., 2014). The BEACHON-RoMBAS measurements were obtained in a ponderosa pine forest and thus were influenced by emissions of biogenic compounds such as α -pinene. CIMS elemental ratios of highly oxidized α -pinene products produced in the PAM reactor agree with ambient measurements within 10%. This suggests that the volatility estimation algorithm successfully captures atmospheric photochemistry of atmospherically relevant SOA precursors, and that our results can be used to interpret ambient measurements in different source regions.

4 Discussion and conclusions

The gas-phase SOA precursors for O_3 and OH oxidation of α -pinene and naphthalene were measured for the first time using a PAM flow reactor and an HR-ToF-CIMS with acetate reagent ion chemistry. The measured organic acid distributions exhibited similarities to gas-phase measurements from previous environmental chamber studies (Yu et al., 1999; Claeys et al., 2013; Kautzman et al., 2009). These measurements extend

6407

the previous measurements to higher OH exposures and include observations of several previously unidentified organic acids, particularly for naphthalene. Particularly they illustrate the concurrent functionalization and fragmentation processes occurring in the gas-phase yielding high and low carbon number acids, the latter dominating the spectra.

In addition, we have presented an approach to estimate the vapor pressures and gas-to-particle partitioning of select organic compounds using HR-ToF-CIMS gas-phase measurements in combination with an algorithm based on the SIMPOL group contribution parameterization method introduced by Pankow and Asher (2008). Previous applications of SIMPOL attempted to use Aerodyne AMS measurements to calculate vapor pressures of organic compounds from their measured elemental ratios (O/C and H/C). However, since functional group information is not available from AMS spectra simplifying assumptions are required which can introduce additional uncertainty (e.g. Donahue et al., 2011). Most recently Yatavelli et al. (2014) applied SIMPOL to MOVI-HR-ToF-CIMS spectra using the acetate reagent ion. They were able to capture the bulk partitioning of species by carbon number by modeling detected compounds as alkanolic acids and adding the remainder of oxygens in the form of different functional groups with hydroxyl groups giving the best agreement. Our approach builds on these studies by incorporating the DBE content of the measured species towards the goal of explicit characterization of oxygen-containing functional groups. This analysis is made possible by the high mass resolution of the TOFWERK HTOF which can resolve the chemical formulas of detected ions.

Our model performs well in predicting the acid contribution to SOA formed from α -pinene ozonolysis compared to previous measurements (Yu et al., 1999; Yatavelli et al., 2012) and to our knowledge, this is the first attempt to estimate the mass of a class of compounds from CIMS spectra using a group contribution model. Semi-explicit model simulations of α -pinene oxidation and SOA formation have agreed with experimental yields within a factor of 2 (Capouet et al., 2008) while models with more degrees of freedom can be tuned to have even greater accuracies (Cappa and Wilson, 2012). Although

6408

- Chemical and microphysical characterization of ambient aerosols with the aerodyne aerosol mass spectrometer, *Mass Spectrom. Rev.*, 26, 185–222, doi:10.1002/mas.20115, 2007. 6388, 6391
- Capouet, M. and Müller, J.-F.: A group contribution method for estimating the vapour pressures of α -pinene oxidation products, *Atmos. Chem. Phys.*, 6, 1455–1467, doi:10.5194/acp-6-1455-2006, 2006. 6405
- Capouet, M., Müller, J. F., Ceulemans, K., Compennolle, S., Vereecken, L., and Peeters, J.: Modeling aerosol formation in alpha-pinene photo-oxidation experiments, *J. Geophys. Res.-Atmos.*, 113, D02308, doi:10.1029/2007JD008995, 2008. 6405, 6408
- Cappa, C. D.: A model of aerosol evaporation kinetics in a thermobalancer, *Atmos. Meas. Tech.*, 3, 579–592, doi:10.5194/amt-3-579-2010, 2010. 6389
- Cappa, C. D. and Jimenez, J. L.: Quantitative estimates of the volatility of ambient organic aerosol, *Atmos. Chem. Phys.*, 10, 5409–5424, doi:10.5194/acp-10-5409-2010, 2010. 6389
- Cappa, C. D. and Wilson, K. R.: Multi-generation gas-phase oxidation, equilibrium partitioning, and the formation and evolution of secondary organic aerosol, *Atmos. Chem. Phys.*, 12, 9505–9528, doi:10.5194/acp-12-9505-2012, 2012. 6395, 6408
- Chan, A. W. H., Kautzman, K. E., Chhabra, P. S., Surratt, J. D., Chan, M. N., Crouse, J. D., Kürten, A., Wennberg, P. O., Flagan, R. C., and Seinfeld, J. H.: Secondary organic aerosol formation from photooxidation of naphthalene and alkylnaphthalenes: implications for oxidation of intermediate volatility organic compounds (IVOCs), *Atmos. Chem. Phys.*, 9, 3049–3060, doi:10.5194/acp-9-3049-2009, 2009. 6392
- Chen, S., Brune, W. H., Lambe, A. T., Davidovits, P., and Onasch, T. B.: Modeling organic aerosol from the oxidation of α -pinene in a Potential Aerosol Mass (PAM) chamber, *Atmos. Chem. Phys.*, 13, 5017–5031, doi:10.5194/acp-13-5017-2013, 2013. 6403
- Chhabra, P. S., Ng, N. L., Canagaratna, M. R., Corrigan, A. L., Russell, L. M., Worsnop, D. R., Flagan, R. C., and Seinfeld, J. H.: Elemental composition and oxidation of chamber organic aerosol, *Atmos. Chem. Phys.*, 11, 8827–8845, doi:10.5194/acp-11-8827-2011, 2011. 6388, 6398
- Claeys, M., Szmigielski, R., Vermeylen, R., Wang, W., Shalamzari, M., and Maenhaut, W.: Tracers for Biogenic Secondary Organic Aerosol from alpha-Pinene and Related Monoterpenes: An Overview, book section 18, NATO Science for Peace and Security Series C: Environmental Security, Springer Netherlands, 227–238, doi:10.1007/978-94-007-5034-0_18, 2013. 6389, 6399, 6407, 6424

6411

- Clegg, S. L., Kleeman, M. J., Griffin, R. J., and Seinfeld, J. H.: Effects of uncertainties in the thermodynamic properties of aerosol components in an air quality model – Part 2: Predictions of the vapour pressures of organic compounds, *Atmos. Chem. Phys.*, 8, 1087–1103, doi:10.5194/acp-8-1087-2008, 2008. 6409
- Compennolle, S., Ceulemans, K., and Müller, J.-F.: Technical Note: Vapor pressure estimation methods applied to secondary organic aerosol constituents from α -pinene oxidation: an intercomparison study, *Atmos. Chem. Phys.*, 10, 6271–6282, doi:10.5194/acp-10-6271-2010, 2010. 6405, 6409
- Daumit, K. E., Kessler, S. H., and Kroll, J. H.: Average chemical properties and potential formation pathways of highly oxidized organic aerosol, *Faraday Discuss.*, 165, 181–202, doi:10.1039/C3FD00045A, 2013. 6395, 6396
- DeCarlo, P. F., Kimmel, J. R., Trimborn, A., Northway, M. J., Jayne, J. T., Aiken, A. C., Gonin, M., Fuhrer, K., Horvath, T., Docherty, K. S., Worsnop, D. R., and Jimenez, J. L.: Field-deployable, high-resolution, time-of-flight aerosol mass spectrometer, *Anal. Chem.*, 78, 8281–8289, doi:10.1021/ac061249n, 2006. 6388, 6391
- Donahue, N. M., Robinson, A. L., Stanier, C. O., and Pandis, S. N.: Coupled partitioning, dilution, and chemical aging of semivolatile organics, *Environ. Sci. Technol.*, 40, 2635–2643, doi:10.1021/es052297c, 2006. 6401
- Donahue, N. M., Epstein, S. A., Pandis, S. N., and Robinson, A. L.: A two-dimensional volatility basis set: 1. organic-aerosol mixing thermodynamics, *Atmos. Chem. Phys.*, 11, 3303–3318, doi:10.5194/acp-11-3303-2011, 2011. 6395, 6408
- Dzepina, K., Cappa, C. D., Volkamer, R. M., Madronich, S., DeCarlo, P. F., Zaveri, R. A., and Jimenez, J. L.: Modeling the multiday evolution and aging of secondary organic aerosol during MILAGRO 2006, *Environ. Sci. Technol.*, 45, 3496–3503, doi:10.1021/es103186f, 2011. 6387
- Eddingsaas, N. C., Loza, C. L., Yee, L. D., Chan, M., Schilling, K. A., Chhabra, P. S., Seinfeld, J. H., and Wennberg, P. O.: α -pinene photooxidation under controlled chemical conditions – Part 2: SOA yield and composition in low- and high- NO_x environments, *Atmos. Chem. Phys.*, 12, 7413–7427, doi:10.5194/acp-12-7413-2012, 2012. 6403
- Ehn, M., Kleist, E., Junninen, H., Petäjä, T., Lönn, G., Schobesberger, S., Dal Maso, M., Trimborn, A., Kulmala, M., Worsnop, D. R., Wahner, A., Wildt, J., and Mentel, Th. F.: Gas phase formation of extremely oxidized pinene reaction products in chamber and ambient air, *Atmos. Chem. Phys.*, 12, 5113–5127, doi:10.5194/acp-12-5113-2012, 2012. 6399

6412

- Ehn, M., Thornton, J. A., Kleist, E., Sipila, M., Junninen, H., Pullinen, I., Springer, M., Rubach, F., Tillmann, R., Lee, B., Lopez-Hilfiker, F., Andres, S., Acir, I.-H., Rissanen, M., Jokinen, T., Schobesberger, S., Kangasluoma, J., Kontkanen, J., Nieminen, T., Kurten, T., Nielsen, L. B., Jorgensen, S., Kjaergaard, H. G., Canagaratna, M., Maso, M. D., Berndt, T., Petaja, T., Wahner, A., Kerminen, V.-M., Kulmala, M., Worsnop, D. R., Wildt, J., and Mentel, T. F.: A large source of low-volatility secondary organic aerosol, *Nature*, 506, 476–479, doi:10.1038/nature13032, 2014. 6405
- Ervens, B., Turpin, B. J., and Weber, R. J.: Secondary organic aerosol formation in cloud droplets and aqueous particles (aqSOA): a review of laboratory, field and model studies, *Atmos. Chem. Phys.*, 11, 11069–11102, doi:10.5194/acp-11-11069-2011, 2011. 6387
- Farmer, D. K., Matsunaga, A., Docherty, K. S., Surratt, J. D., Seinfeld, J. H., Ziemann, P. J., and Jimenez, J. L.: Response of an aerosol mass spectrometer to organonitrates and organosulfates and implications for atmospheric chemistry, *P. Natl. Acad. Sci. USA*, 107, 6670–6675, doi:10.1073/pnas.0912340107, 2010. 6388
- Goldstein, A. H. and Galbally, I. E.: Known and unexplored organic constituents in the earth's atmosphere, *Environ. Sci. Technol.*, 41, 1514–1521, doi:10.1021/es072476p, 2007. 6386, 6387
- Hallquist, M., Wenger, J. C., Baltensperger, U., Rudich, Y., Simpson, D., Claeys, M., Dommen, J., Donahue, N. M., George, C., Goldstein, A. H., Hamilton, J. F., Herrmann, H., Hoffmann, T., Iinuma, Y., Jang, M., Jenkin, M. E., Jimenez, J. L., Kiendler-Scharr, A., Maenhaut, W., McFiggans, G., Mentel, Th. F., Monod, A., Prévôt, A. S. H., Seinfeld, J. H., Surratt, J. D., Szmigielski, R., and Wildt, J.: The formation, properties and impact of secondary organic aerosol: current and emerging issues, *Atmos. Chem. Phys.*, 9, 5155–5236, doi:10.5194/acp-9-5155-2009, 2009. 6387
- Heald, C. L., Kroll, J. H., Jimenez, J. L., Docherty, K. S., DeCarlo, P. F., Aiken, A. C., Chen, Q., Martin, S. T., Farmer, D. K., and Artaxo, P.: A simplified description of the evolution of organic aerosol composition in the atmosphere, *Geophys. Res. Lett.*, 37, L08803, doi:10.1029/2010GL042737, 2010. 6387
- Herndon, S. C., Zahniser, M. S., Nelson, D. D., Shorter, J., McManus, J. B., Jiménez, R., Warneke, C., and de Gouw, J. A.: Airborne measurements of HCHO and HCOOH during the New England Air Quality Study 2004 using a pulsed quantum cascade laser spectrometer, *J. Geophys. Res.-Atmos.*, 112, D10S03, doi:10.1029/2006JD007600, 2007. 6391

6413

- Hilal, S. H., Carreira, A., and Karikhoff, S. W.: Estimation of Chemical Reactivity Parameters and Physical Properties of Organic Molecules using SPARC, book section 9, 1 edn., Elsevier, 291–353, 1994. 6409
- Huffman, J. A., Docherty, K. S., Aiken, A. C., Cubison, M. J., Ulbrich, I. M., DeCarlo, P. F., Sueper, D., Jayne, J. T., Worsnop, D. R., Ziemann, P. J., and Jimenez, J. L.: Chemically-resolved aerosol volatility measurements from two megacity field studies, *Atmos. Chem. Phys.*, 9, 7161–7182, doi:10.5194/acp-9-7161-2009, 2009. 6389, 6406
- Jayne, J. T., Leard, D. C., Zhang, X., Davidovits, P., Smith, K. A., Kolb, C. E., and Worsnop, D. R.: Development of an Aerosol Mass Spectrometer for Size and Composition Analysis of Submicron Particles, *Aerosol Sci. Tech.*, 33, 49–70, doi:10.1080/027868200410840, 2000. 6388
- Jimenez, J. L., Canagaratna, M. R., Donahue, N. M., Prevot, A. S. H., Zhang, Q., Kroll, J. H., DeCarlo, P. F., Allan, J. D., Coe, H., Ng, N. L., Aiken, A. C., Docherty, K. S., Ulbrich, I. M., Grieshop, A. P., Robinson, A. L., Duplissy, J., Smith, J. D., Wilson, K. R., Lanz, V. A., Hueglin, C., Sun, Y. L., Tian, J., Laaksonen, A., Raatikainen, T., Rautiainen, J., Vaattovaara, P., Ehn, M., Kulmala, M., Tomlinson, J. M., Collins, D. R., Cubison, M. J., E., Dunlea, J., Huffman, J. A., Onasch, T. B., Alfarra, M. R., Williams, P. I., Bower, K., Kondo, Y., Schneider, J., Drewnick, F., Borrmann, S., Weimer, S., Demerjian, K., Salcedo, D., Cottrell, L., Griffin, R., Takami, A., Miyoshi, T., Hatakeyama, S., Shimono, A., Sun, J. Y., Zhang, Y. M., Dzepina, K., Kimmel, J. R., Sueper, D., Jayne, J. T., Herndon, S. C., Trimborn, A. M., Williams, L. R., Wood, E. C., Middlebrook, A. M., Kolb, C. E., Baltensperger, U., and Worsnop, D. R.: Evolution of organic aerosols in the atmosphere, *Science*, 326, 1525–1529, doi:10.1126/science.1180353, 2009. 6386, 6387
- Kang, E., Root, M. J., Toohey, D. W., and Brune, W. H.: Introducing the concept of Potential Aerosol Mass (PAM), *Atmos. Chem. Phys.*, 7, 5727–5744, doi:10.5194/acp-7-5727-2007, 2007. 6391
- Kautzman, K. E., Surratt, J. D., Chan, M. N., Chan, A. W. H., Hersey, S. P., Chhabra, P. S., Dalleska, N. F., Wennberg, P. O., Flagan, R. C., and Seinfeld, J. H.: Chemical composition of gas- and aerosol-phase products from the photooxidation of naphthalene, *J. Phys. Chem. A*, 114, 913–934, doi:10.1021/jp908530s, 2009. 6389, 6400, 6404, 6407, 6423, 6424
- Kessler, S. H., Smith, J. D., Che, D. L., Worsnop, D. R., Wilson, K. R., and Kroll, J. H.: Chemical sinks of organic aerosol: kinetics and products of the heterogeneous oxidation of erythritol and levoglucosan, *Environ. Sci. Technol.*, 44, 7005–7010, doi:10.1021/es101465m, 2010. 6395

6414

- Kessler, S. H., Nah, T., Daumit, K. E., Smith, J. D., Leone, S. R., Kolb, C. E., Worsnop, D. R., Wilson, K. R., and Kroll, J. H.: OH-initiated heterogeneous aging of highly oxidized organic aerosol, *J. Phys. Chem. A*, 116, 6358–6365, doi:10.1021/jp212131m, 2012. 6395
- Kroll, J. H. and Seinfeld, J. H.: Chemistry of secondary organic aerosol: Formation and evolution of low-volatility organics in the atmosphere, *Atmos. Environ.*, 42, 3593–3624, doi:10.1016/j.atmosenv.2008.01.003, 2008. 6387
- Kroll, J. H., Smith, J. D., Che, D. L., Kessler, S. H., Worsnop, D. R., and Wilson, K. R.: Measurement of fragmentation and functionalization pathways in the heterogeneous oxidation of oxidized organic aerosol, *Phys. Chem. Chem. Phys.*, 11, 8005–8014, doi:10.1039/B905289E, 2009. 6393, 6400, 6404
- Kroll, J. H., Donahue, N. M., Jimenez, J. L., Kessler, S. H., Canagaratna, M. R., Wilson, K. R., Altieri, K. E., Mazzoleni, L. R., Wozniak, A. S., Bluhm, H., Mysak, E. R., Smith, J. D., Kolb, C. E., and Worsnop, D. R.: Carbon oxidation state as a metric for describing the chemistry of atmospheric organic aerosol, *Nat. Chem.*, 3, 133–139, 2011. 6400
- Kundu, S., Fisseha, R., Putman, A. L., Rahn, T. A., and Mazzoleni, L. R.: High molecular weight SOA formation during limonene ozonolysis: insights from ultrahigh-resolution FT-ICR mass spectrometry characterization, *Atmos. Chem. Phys.*, 12, 5523–5536, doi:10.5194/acp-12-5523-2012, 2012. 6387
- Lambe, A. T., Ahern, A. T., Williams, L. R., Slowik, J. G., Wong, J. P. S., Abbatt, J. P. D., Brune, W. H., Ng, N. L., Wright, J. P., Croasdale, D. R., Worsnop, D. R., Davidovits, P., and Onasch, T. B.: Characterization of aerosol photooxidation flow reactors: heterogeneous oxidation, secondary organic aerosol formation and cloud condensation nuclei activity measurements, *Atmos. Meas. Tech.*, 4, 445–461, doi:10.5194/amt-4-445-2011, 2011a. 6391, 6393, 6403, 6429
- Lambe, A. T., Onasch, T. B., Massoli, P., Croasdale, D. R., Wright, J. P., Ahern, A. T., Williams, L. R., Worsnop, D. R., Brune, W. H., and Davidovits, P.: Laboratory studies of the chemical composition and cloud condensation nuclei (CCN) activity of secondary organic aerosol (SOA) and oxidized primary organic aerosol (OPOA), *Atmos. Chem. Phys.*, 11, 8913–8928, doi:10.5194/acp-11-8913-2011, 2011b. 6398, 6404, 6406
- Lambe, A. T., Onasch, T. B., Croasdale, D. R., Wright, J. P., Martin, A. T., Franklin, J. P., Massoli, P., Kroll, J. H., Canagaratna, M. R., Brune, W. H., Worsnop, D. R., and Davidovits, P.: Transitions from functionalization to fragmentation reactions of laboratory Secondary Organic

6415

- Aerosol (SOA) generated from the OH oxidation of alkane precursors, *Environ. Sci. Technol.*, 46, 5430–5437, doi:10.1021/es300274t, 2012. 6393, 6400, 6404
- Laskin, A., Laskin, J., and Nizkorodov, S. A.: Mass spectrometric approaches for chemical characterisation of atmospheric aerosols: critical review of the most recent advances, *Environ. Chem.*, 9, 163–189, doi:10.1071/EN12052, 2012. 6387
- Lee, A., Goldstein, A. H., Keywood, M. D., Gao, S., Varutbangkul, V., Bahreini, R., Ng, N. L., Flagan, R. C., and Seinfeld, J. H.: Gas-phase products and secondary aerosol yields from the ozonolysis of ten different terpenes, *J. Geophys. Res.-Atmos.*, 111, D07302, doi:10.1029/2005JD006437, 2006. 6399
- Lim, Y. B., Tan, Y., Perri, M. J., Seitzinger, S. P., and Turpin, B. J.: Aqueous chemistry and its role in secondary organic aerosol (SOA) formation, *Atmos. Chem. Phys.*, 10, 10521–10539, doi:10.5194/acp-10-10521-2010, 2010. 6387
- Lopez-Hilfiker, F. D., Mohr, C., Ehn, M., Rubach, F., Kleist, E., Wildt, J., Mentel, Th. F., Lutz, A., Hallquist, M., Worsnop, D., and Thornton, J. A.: A novel method for online analysis of gas and particle composition: description and evaluation of a Filter Inlet for Gases and AEROSols (FIGAERO), *Atmos. Meas. Tech.*, 7, 983–1001, doi:10.5194/amt-7-983-2014, 2014. 6409
- Mao, J., Ren, X., Brune, W. H., Olson, J. R., Crawford, J. H., Fried, A., Huey, L. G., Cohen, R. C., Heikes, B., Singh, H. B., Blake, D. R., Sachse, G. W., Diskin, G. S., Hall, S. R., and Shetter, R. E.: Airborne measurement of OH reactivity during INTEX-B, *Atmos. Chem. Phys.*, 9, 163–173, doi:10.5194/acp-9-163-2009, 2009. 6392
- Mazzoleni, L. R., Ehrmann, B. M., Shen, X., Marshall, A. G., and Collett, J. L.: Water-soluble atmospheric organic matter in fog: exact masses and chemical formula identification by ultrahigh-resolution fourier transform ion cyclotron resonance mass spectrometry, *Environ. Sci. Technol.*, 44, 3690–3697, doi:10.1021/es903409k, 2010. 6387
- Mohr, C., Lopez-Hilfiker, F. D., Zotter, P., Prévôt, A. S. H., Xu, L., Ng, N. L., Herndon, S. C., Williams, L. R., Franklin, J. P., Zahniser, M. S., Worsnop, D. R., Knighton, W. B., Aiken, A. C., Gorkowski, K. J., Dubey, M. K., Allan, J. D., and Thornton, J. A.: Contribution of nitrated phenols to wood burning brown carbon light absorption in detling, United Kingdom during winter time, *Environ. Sci. Technol.*, 47, 6316–6324, doi:10.1021/es400683v, 2013. 6388
- Moldoveanu, S. C.: Pyrolysis of carboxylic acids, in: *Techniques and Instrumentation in Analytical Chemistry*, Vol. 28, book section 17, Elsevier, 471–526, doi:10.1016/S0167-9244(09)02817-0, 2010. 6406

6416

- Yatavelli, R. L. N. and Thornton, J. A.: Particulate organic matter detection using a micro-orifice volatilization impactor coupled to a chemical ionization mass spectrometer (MOVI-CIMS), *Aerosol Sci. Tech.*, 44, 61–74, doi:10.1080/02786820903380233, 2010. 6409
- Yatavelli, R. L. N., Lopez-Hilfiker, F., Wargo, J. D., Kimmel, J. R., Cubison, M. J., Bertram, T. H., Jimenez, J. L., Gonin, M., Worsnop, D. R., and Thornton, J. A.: A chemical ionization high-resolution time-of-flight mass spectrometer coupled to a micro orifice volatilization impactor (movi-hrtf-cims) for analysis of gas and particle-phase organic species, *Aerosol Sci. Tech.*, 46, 1313–1327, doi:10.1080/02786826.2012.712236, 2012. 6388, 6390, 6391, 6398, 6403, 6404, 6408, 6422
- Yatavelli, R. L. N., Stark, H., Thompson, S. L., Kimmel, J. R., Cubison, M. J., Day, D. A., Campuzano-Jost, P., Palm, B. B., Hodzic, A., Thornton, J. A., Jayne, J. T., Worsnop, D. R., and Jimenez, J. L.: Semicontinuous measurements of gas–particle partitioning of organic acids in a ponderosa pine forest using a MOVI-HRToF-CIMS, *Atmos. Chem. Phys.*, 14, 1527–1546, doi:10.5194/acp-14-1527-2014, 2014. 6388, 6406, 6407, 6408, 6429
- Yu, J., Cocker, David R., Griffin, R., Flagan, R., and Seinfeld, J.: Gas-phase ozone oxidation of monoterpenes: gaseous and particulate products, *J. Atmos. Chem.*, 34, 207–258, doi:10.1023/A:1006254930583, 1999. 6389, 6399, 6403, 6404, 6407, 6408, 6423, 6424
- Zahardis, J., Geddes, S., and Petrucci, G. A.: Improved understanding of atmospheric organic aerosols via innovations in soft ionization aerosol mass spectrometry, *Anal. Chem.*, 83, 2409–2415, doi:10.1021/ac102737k, 2011. 6388
- Zhang, Q., Jimenez, J. L., Canagaratna, M. R., Allan, J. D., Coe, H., Ulbrich, I., Alfarra, M. R., Takami, A., Middlebrook, A. M., Sun, Y. L., Dzepina, K., Dunlea, E., Docherty, K., DeCarlo, P. F., Salcedo, D., Onasch, T., Jayne, J. T., Miyoshi, T., Shimojo, A., Hatakeyama, S., Takegawa, N., Kondo, Y., Schneider, J., Drewnick, F., Borrmann, S., Weimer, S., Demerjian, K., Williams, P., Bower, K., Bahreini, R., Cottrell, L., Griffin, R. J., Rautiainen, J., Sun, J. Y., Zhang, Y. M., and Worsnop, D. R.: Ubiquity and dominance of oxygenated species in organic aerosols in anthropogenically-influenced Northern Hemisphere midlatitudes, *Geophys. Res. Lett.*, 34, L13801, doi:10.1029/2007GL029979, 2007. 6386, 6402

6419

Table 1. Experimental conditions and results.

Expt.#	VOC System	VOC Conc. (ppb)	OH Exposure (molec cm ⁻³ s)	OH Days ^a	\bar{n}_c^b	$\overline{O/C}^c$	$\overline{H/C}^d$	\overline{OS}_c^e
1	α -pinene + O ₃	15	–	–	3.57	0.81	1.45	0.18
2	α -pinene + O ₃	30	–	–	4.31	0.70	1.46	–0.05
3	α -pinene + OH	15	3.7×10^{11}	2.8	3.52	0.88	1.38	0.39
4	α -pinene + OH	15	7.0×10^{11}	5.4	3.06	1.01	1.33	0.69
5	α -pinene + OH	30	7.0×10^{11}	5.4	3.25	0.98	1.32	0.64
6	α -pinene + OH	30	9.7×10^{11}	7.5	3.27	1.00	1.31	0.69
7	α -pinene + OH	15	9.7×10^{11}	7.5	3.13	0.99	1.31	0.68
8	naphthalene + OH	23 ^f	1.2×10^{11}	0.96	3.57	0.99	1.29	0.69
9	naphthalene + OH	46 ^f	1.2×10^{11}	0.96	5.00	0.75	1.18	0.31
10	naphthalene + OH	46 ^f	1.2×10^{11}	0.96	4.60	0.84	1.27	0.40
11	naphthalene + OH	23 ^f	1.9×10^{11}	1.5	4.51	0.84	1.27	0.40
12	naphthalene + OH	23 ^f	2.8×10^{11}	2.1	4.54	0.79	1.16	0.41
13	naphthalene + OH	23 ^f	3.7×10^{11}	2.8	3.47	0.93	1.15	0.71
14	naphthalene + OH	23 ^f	5.3×10^{11}	4.1	2.94	1.06	1.20	0.92
15	naphthalene + OH	23 ^f	9.7×10^{11}	7.5	2.88	1.07	1.21	0.93

^a Based on a diurnally averaged OH concentration of 1.5×10^6 molec cm⁻³.^b Average carbon number.^c Average oxygen-to-carbon ratio.^d Average hydrogen-to-carbon ratio.^e Average carbon oxidation state.^f Concentration estimated from equilibrium vapor pressure at 25 °C.

6420

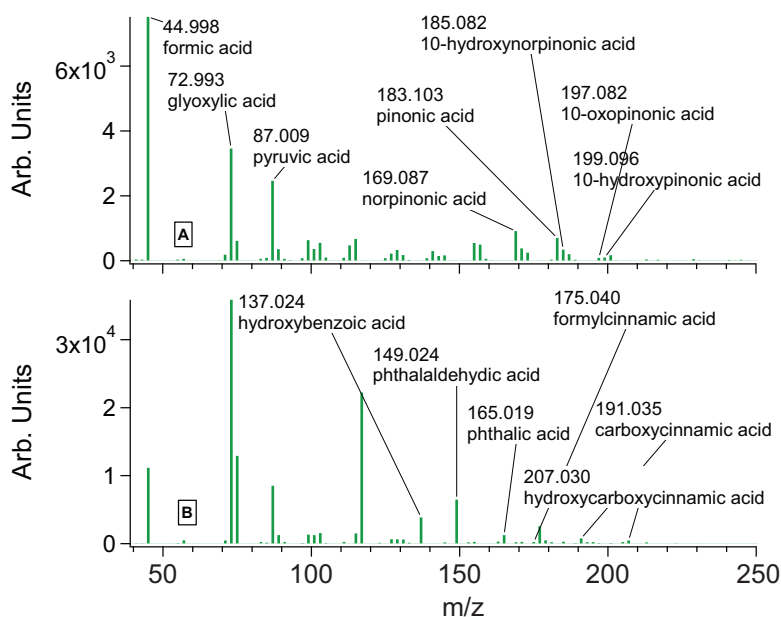


Figure 2. Acetate-CIMS unit mass resolution spectra of α -pinene ozonolysis (**A**, Expt. 1), and naphthalene photooxidation (**B**, Expt. 12). Even massed ions, reagent ions, and dominant background ions are removed, and blank spectra are subtracted. Select ions identified in previous studies are labeled (Yu et al., 1999; Kautzman et al., 2009).

6423

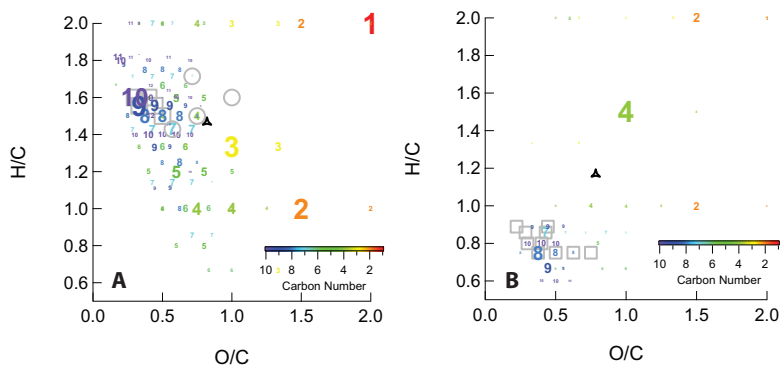


Figure 3. Modified Van Krevelen diagram of gas-phase acetate-CIMS high-resolution spectra of (**A**) α -pinene ozonolysis (Expt. 1) and (**B**) naphthalene photooxidation (Expt. 12). Each integer marker represents a fitted ion with the number representing the carbon number of the ion. The colorscale is representative of the carbon number range of the HR spectrum. The size of each number is proportional to the carbon number weighted signal of its corresponding ion; the largest markers in (**A**) and (**B**) represent 8.8% and 38% of the carbon weighted signal, respectively. Gray square markers in (**A**) indicate tracer acids identified by Yu et al. (1999) and gray circle markers indicate SOA tracer acids noted in Claeys et al. (2013). Gray square markers in (**B**) indicate tracer acids identified by Kautzman et al. (2009). Names and locations of acids on the VK are shown in Supplement, Figs. 3 and 4. The bulk O/C and H/C values are marked by black triangles.

6424

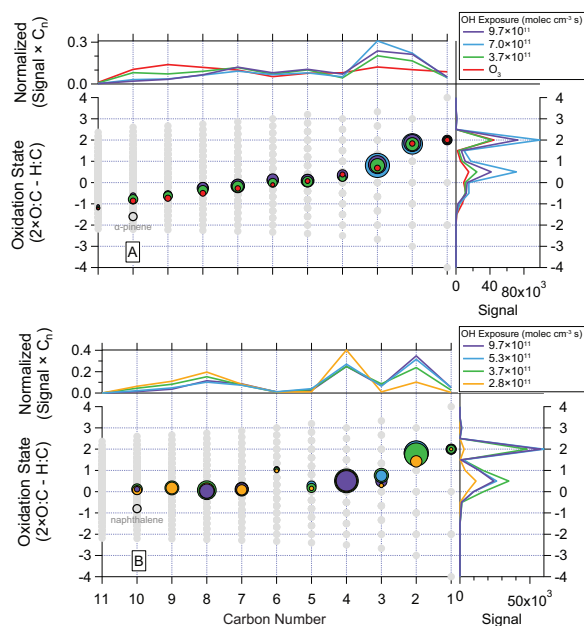


Figure 4. Kroil diagram for α -pinene (**A**) and naphthalene (**B**) oxidation experiments. The main panel displays the average OS_C per carbon number for each oxidation experiment. The area of the marker is proportional to the signal times the carbon number. The top panel plots the fraction of carbon weighted signal at each carbon number. The right panel displays the signal distribution across oxidation state.

6425

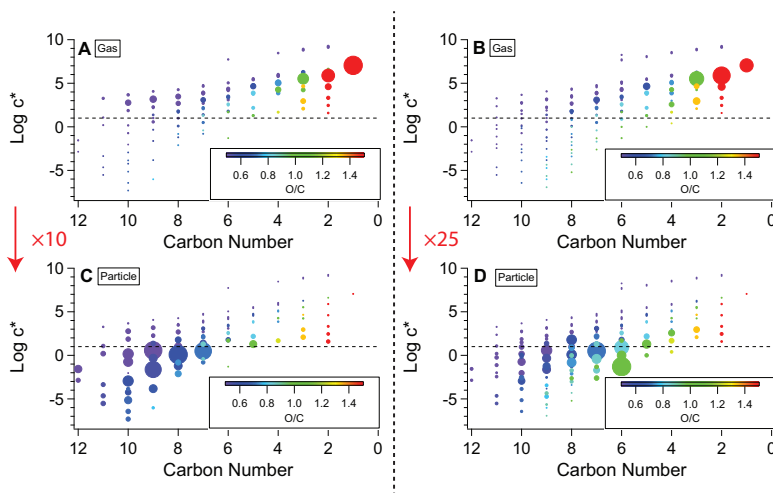


Figure 5. Estimated $\log c^*$ as a function of carbon number and O/C. (**A**) and (**C**) represent extracted gas and particle spectra of α -pinene ozonolysis (Expt. 1), respectively, and (**B**) and (**D**) represent the same of α -pinene photooxidation at high OH exposures (Expt. 7). Marker area is proportional to the fraction of mass in the depicted spectra. The factor and arrow in red represents the relative mass scale between gas and particle spectra. For example $\times 10$ between (**A**) and (**C**) indicate that markers of equal area represent 10 times more mass in the gas-phase spectrum.

6426

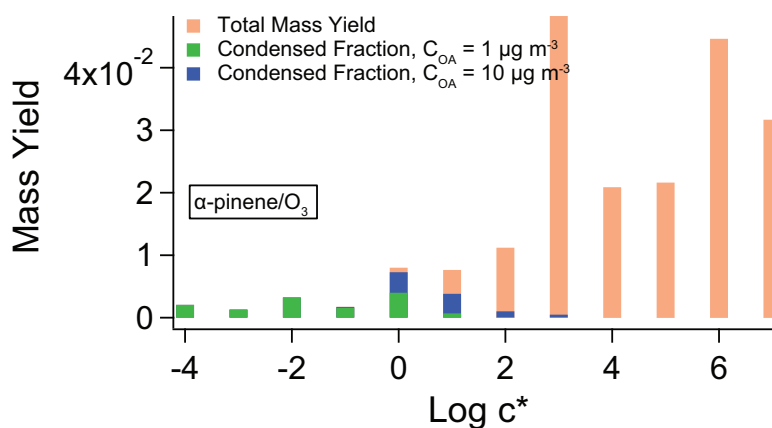


Figure 6. Estimated mass yield of compounds measured by the acetate-CIMS for α -pinene ozonolysis (Expt. 1), binned by $\log c^*$. Colored in green is the fraction that would condense with $C_{\text{OA}} = 1 \mu\text{g m}^{-3}$ and colored in blue is the additional mass that would condense with $C_{\text{OA}} = 10 \mu\text{g m}^{-3}$.

6427

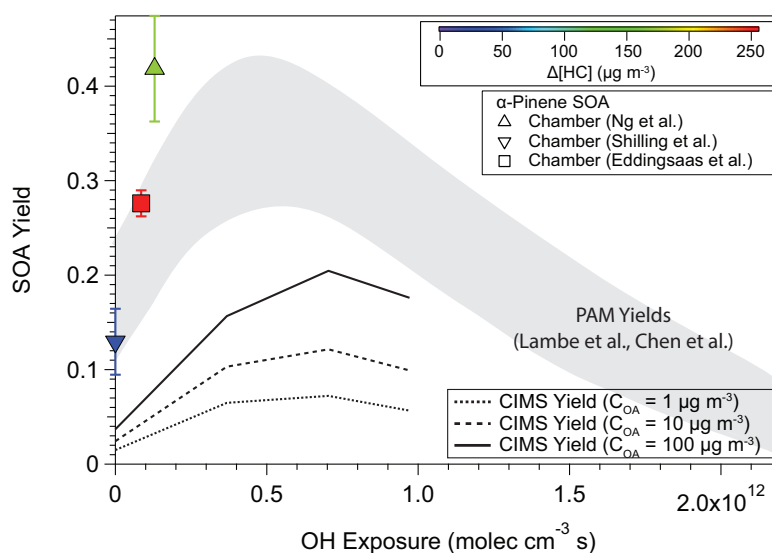


Figure 7. SOA yields estimated by the acetate-CIMS in this study and previously reported SOA yields from SMPS measurements for α -pinene oxidation systems. The dotted black lines depict CIMS yields calculated for $C_{\text{OA}} = 1, 10, \text{ and } 100 \mu\text{g m}^{-3}$. The gray shaded region represents the domain of yields determined from PAM experiments across OH exposure where the amount of α -pinene reacted ranged from 227 to 556 $\mu\text{g m}^{-3}$. Zero OH exposure corresponds to ozonolysis. Square and triangle points indicate yields determined from chamber experiments; their colors are indicative of the amount of α -pinene reacted.

6428

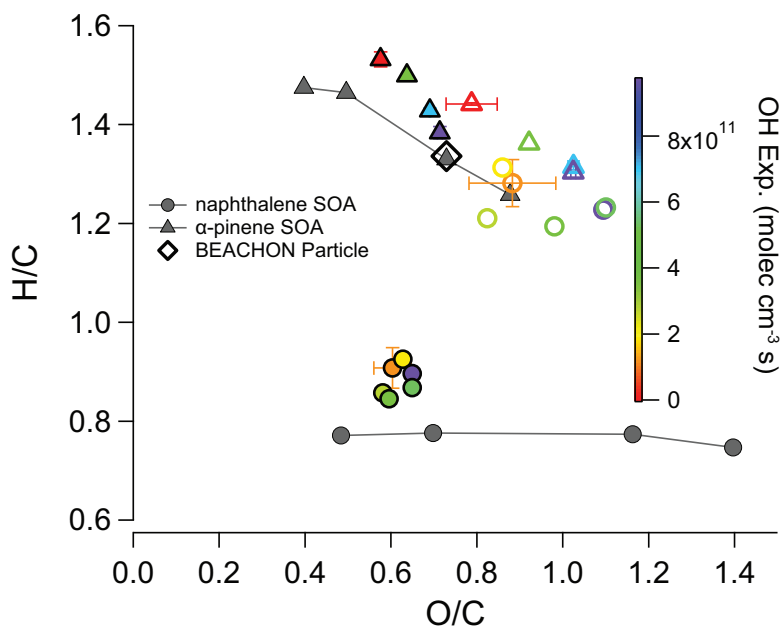


Figure 8. Average O/C and H/C ratios for extracted particle-phase (solid colored markers) and gas-phase (outlined colored markers) acetate-CIMS spectra as a function of OH exposure. Gray points represent AMS elemental ratios from Lambe et al. (2011a). Average particle-phase elemental ratios from the BEACHON-RoMBAS field campaign obtained from MOVI-HRToF-CIMS measurements are depicted by a black diamond (Yatavelli et al., 2014; Ortega et al., 2014).